Journal of Statistics Applications & Probability
An International Journal

http://dx.doi.org/10.18576/jsap/140610

Optimizing Conjugate Gradient Methods for Image Recovery from Salt and Pepper Noise

Basim A. Hassan[1] *and Talal Alharbi*[2,*]

[1]Department of Mathematics, College of Computers Sciences and Mathematics, University of Mosul, Iraq
[2]Department of Mathematic, College of Science, Qassim University, Buraydah 52571, Saudi Arabia

Received: 19 Sep. 2025, Revised: 5 Oct. 2025, Accepted: 6 Oct. 2025
Published online: 1 Nov. 2025

Abstract: This study focuses on image restoration from salt-and-pepper impulse noise using an enhanced Conjugate Gradient (CG) method. The proposed approach adopts a two-phase process: first, an adaptive median filter identifies corrupted pixels; second, a smooth optimization problem replaces a non-smooth one to reconstruct the image. New formulas derived from the Taylor series are introduced to define the BBY algorithms, which improve convergence and maintain essential image features like edges. The convergence analysis demonstrates that the proposed methods satisfy descent conditions and are globally convergent. Experimental results using standard images (e.g., Lena, House, Elaine, Cameraman) show that BBY algorithms outperform the classical FR method in both computational efficiency and image quality, measured using PSNR. Numerical comparisons reveal lower iteration counts and higher PSNR values for BBY. Theoretical assumptions are validated with practical experiments. The BBY framework proves robust and effective for real-world noisy image restoration. Overall, the study demonstrates the strength of combining optimization theory with practical image processing techniques.

Keywords: Optimization Algorithm, impulse noise, two-phase approach, Global Optimization, Conjugate Gradient (CG) method and convergence.

1 Introduction

Since noise poses a challenge, the image degradation needs sophisticated restoration approaches to extract the original image. Impulse noise, especially salt and pepper noise is widespread among all the different types of noise there are in digital imaging and is one of the most difficult to deal with [1,2]. It is defined as the random presence of extreme pixel values resulting in white and black pixel sparsely scattered throughout the image. Letting maximum intensity value pixels become mistakenly set to the most value roughly characterizes salt noise [3]. For example, pepper noise occurs when low intensity pixels are set to zero [4,5]. The image restoration area has come a long way from heuristic filtering algorithms to optimization-based and model-based approaches.

Initial approaches heavily relied on spatial domain filters, which acted directly on pixel values of an image. Among those, the median filter is one of the extremely useful and common non-linear impulse noise filters to eliminate noises. The overall idea of the median filter is to replace a central pixel value with the median value of pixel values in its provided neighborhood. The operation is especially well suited to edge preservation but highly effective in smoothing impulsively occurring outliers since the median is less sensitive to outliers than the mean employed in linear filters [6,7].

Large-scale systems of linear equations and unconstrained optimization problems, especially those resulting from the discretization of partial differential equations, which are frequently encountered in image processing and computer vision, are frequently solved using the Conjugate Gradient (CG) method [8], a potent iterative optimization algorithm. For large systems where direct inversion is computationally prohibitive, it is a highly efficient alternative to direct methods due to its strong convergence properties for general non-linear functions and its ability to converge in a finite number of steps for quadratic functions in exact arithmetic [9,10].

In this study, the proposed conjugate gradient algorithm is employed to address challenges in image restoration. Raymond et al. [11] proposed a two-step approach to the recovery of noisy impulse images; in the initial step, they

* Corresponding author e-mail: Ta.alharbi@qu.edu.sa

employed a median filter to identify and separate noisy pixels. Consider an image X of size $M \times N$, with every pixel position addressed by the index set $A = \{1,2,\dots,M\} \times \{1,2,\dots,N\}$. Let $|N|$ be the number of pixels detected as noisy pixels during the first-pass detection and let $N \subset A$ be the set of noisy pixel indices. For any pixel located at position $(m,n) \in A$, the set of its four nearest neighboring pixels is denoted by B_{mn}. Furthermore, let $y_{m,n}$ denote the observed intensity value at pixel position (m,n).

In the second stage of the restoration process, the recovery of the corrupted pixels is formulated as a nonsmooth optimization problem, which aims to accurately reconstruct the original pixel intensities:

$$\min_q \sum_{(m,n)\in N} \left[|q_{m,n} - y_{m,a}| + \frac{\beta}{2}(2 \cdot Z^1_{m,s} + Z^2_{m,n}) \right], \tag{1}$$

where:

$$Z^1_{m,n} = \sum_{(a,b)\in B_{m,N}} \psi_a(q_{m,n} - y_{a,h}), \quad Z^2_{m,n} = \sum_{(a,b)\in B_{m,n} \sim N} \psi_a(q_{a,n} - q_{a,b}), \tag{2}$$

The function $\psi_\sigma(t) = \sqrt{t^2 + \alpha}$, where $\alpha > 0$ is a parameter, serves as an edge-preserving regularization term. This function is particularly important for noise removal tasks that aim to maintain significant image features [12,13], such as edges. The vector $q = [q_{m,n}]_{(m,n)\in V}$ is defined as a length-based column vector, with the set $|N|$ arranged in lexicographic order.

Solving the nonsmooth minimization problem presented in equation (1) exactly is computationally intensive and time-consuming. To address this, Cai et al. [2] proposed a method that eliminates the nonsmooth term, resulting in the following smooth and unconstrained optimization problem:

$$\min_q f_a(x) := \sum_{(m,n)\in N} \left(2 \sum_{(a,b)\in B_{m,n}|N} \psi_a(q_{m,n} - y_{a,b}) + \sum_{(a,b)\in B_{m,n}\cap N} \psi_a(q_{m,n} - q_{a,b}) \right). \tag{3}$$

The complexity of problem (3) increases proportionally with the noise level. Employing the Conjugate Gradient (CG) method to solve the optimization problem (3), the authors in [15] demonstrated effective restoration of corrupted images.

In the present study, salt-and-pepper noise, a specific type of impulse noise, is addressed using a two-phase approach [16]. During the first phase, noisy pixels are detected via an adaptive median filter as described in [17]. Subsequently, the problem (3) is solved using the proposed BBY algorithms, and its performance is benchmarked against FR method from [18,19].

In conjugate gradient methods, the new point x_{k+1} is computed iteratively using both the current point x_k and a search direction d_k that is conjugate to the previous directions [20,21]. The general update rule is given by:

$$x_{k+1} = x_k + \alpha_k d_k, \tag{4}$$

where α_k is the step size, which is known as:

$$\alpha_k = -\frac{g_k^T d_k}{d_k^T G d_k}, \tag{5}$$

see [22]. More generally, α_k is often determined using a line search method that satisfies the Wolfe conditions as:

$$f(u_k + \alpha_k d_k) \le f(u_k) + \delta \cdot \alpha_k g_k^T d_k, \tag{6}$$

$$d_k^T g(u_k + \alpha_k d_k) \ge \sigma \cdot d_k^T g_k, \tag{7}$$

where $0 < \delta < \sigma < 1$ [23]. d_k is the current conjugate direction, updated as follows:

$$d_{k+1} = -g_{k+1} + \beta_k \cdot d_k, \tag{8}$$

where g_{k+1} is the gradient of the objective function at iteration $k+1$, and β_k is a scalar that controls how much of the previous direction is preserved in the current iteration. One of the most commonly used formulas for computing β_k is the Fletcher–Reeves (FR) [24] formula:

$$\beta_k^{FR} = \frac{g_{k+1}^T g_{k+1}}{g_k^T g_k}, \tag{9}$$

This formula ensures that the directions d_k remain conjugate with respect to the Hessian matrix (in the case of quadratic functions), which leads to faster convergence than simple steepest descent methods. The conjugate gradient method is especially effective for large-scale problems, where storing or inverting the Hessian matrix is impractical.

The study placed a strong focus on harnessing the dual benefits–computational performance and theoretical rigor–provided by new conjugate gradient approaches.

2 Deriving new parameters via the Taylor series

We propose several new formulas for the gradient method derived using the Taylor series as follows:

$$f(x_k) = f(x_{k+1}) - g_k^T s_k + \frac{1}{2} s_k^T Q(x_k) s_k, \tag{10}$$

To compute the derivative, we use the following formula:

$$g_{k+1} = g_k + Q(u_{k+1}) s_k, \tag{11}$$

From the relationships established in (11) and (10), it follows that:

$$s_k^T Q(u_{k+1}) s_k = \frac{3}{2} s_k^T y_k + (f_{k+1} - f_k), \tag{12}$$

Thus, following some algebraic transformations, we derive the expression:

$$s_k^T Q(x_k) s_k = \frac{3}{2} \frac{(g_k^T s_k)^2}{s_k^T y_k + (f_k - f_{k+1})} = \omega_k^1 s_k^T y_k, \tag{13}$$

where:

$$\omega_k^1 = \frac{3}{2} \frac{(g_k^T s_k)^2}{s_k^T y_k (s_k^T y_k + (f_k - f_{k+1}))}, \tag{14}$$

The conjugacy condition is known to be defined by the following relation, which plays a key role in the analysis:

$$d_{k+1}^T Q s_k = 0, \tag{15}$$

After simplifying (13) algebraically and inserting it into (15), we get the following result:

$$\beta_k = \omega_k \frac{g_{k+1}^T y_k}{d_k^T y_k}, \tag{16}$$

Assuming exact line search is utilized in both (12) and (16), the outcome is:

$$\beta_k = \omega_k \frac{\|g_{k+1}\|^2}{d_k^T y_k}, \tag{17}$$

with:

$$\omega_k^2 = \frac{3}{2} \frac{(g_k^T s_k)^2}{s_k^T y_k (-s_k^T g_k + (f_k - f_{k+1}))}, \tag{18}$$

and

$$\omega_k^3 = \frac{3}{2} \frac{(g_k^T s_k)^2}{s_k^T y_k (\alpha_k g_k^T g_k + (f_k - f_{k+1}))}. \tag{19}$$

The proposed methods BBY is clearly defined and offers a robust framework to improve convergence and algorithm performance [25].

They are referred to as BBY for convenience.

Algorithm BBY:

Input: Minimize a function by adjusting $x_0 \in \mathbb{R}^n$, ε.

Output: Optimal x with near-zero gradient.

1.If $\|g_k\| < \varepsilon$ stop.
2.Compute α_k using (6) and (7).
3.Update $x_{k+1} = x_k + \alpha_k d_k$ and compute β_k using (17) with (14, 18, and 19).
4.Calculate $d_{k+1} = -g_{k+1} + \beta_k s_k$.
5.Increment the iteration counter: $k = k+1$ and return to step 2.

Theoretical foundations of BBY algorithms and many advanced Conjugate Gradient methods are based on basic ideas of numerical optimization, especially when it comes to descent conditions and global convergence. Constitute the theoretical basis for BBY algorithms and, in reality, several advanced Conjugate Gradient methods [26]. The most important efficiency hypotheses of BBY algorithms are image quality and computation velocity. It is a fundamental argument that BBY algorithms have an advantage over the conventional Fletcher-Reeves (FR) method in terms of both image quality and computation efficiency. To serve as a reference, the FR algorithm–one of the earliest and most widely used nonlinear Conjugate Gradient algorithms–is used [27].

3 Convergence analysis

Assumptions required for the proof of the convergence property:

1. The set $L_0 = \{x \in \mathbb{R}^n : f(x) \leq f(x_0)\}$ is assumed to be convex [28].
2. The gradient ∇f is Lipschitz continuous: $(\nabla f(o) - \nabla f(v)) \leq L\|o - v\|$ for all $o, v \in \mathbb{R}^n$.

The next theorem establishes that the new algorithm fulfills the descent condition.

Theorem 3.1. Suppose the sequence $\{x_k\}$ is computed based on the parameters in (3) and (17). Then

$$d_{k+1}^T g_{k+1} < 0 \quad \text{and} \quad d_{k+1}^T g_{k+1} = \beta_k d_k^T g_k. \tag{20}$$

Proof. Equation (3) multiplied by g_{k+1}^T results in:

$$d_{k+1}^T g_{k+1} = -g_{k+1}^T g_{k+1} + \beta_k^{BBY1} d_k^T g_{k+1}, \tag{21}$$

Thus, equation (21) implies:

$$\|g_{k+1}\|^2 = \frac{\beta_k^{BBY1} d_k^T y_k}{\frac{3}{2}\frac{(g_k^T s_k)^2}{s_k^T y_k (s_k^T y_k + (f_k - f_{k+1}))}}. \tag{22}$$

Equations (21) and (22) are now used to get:

$$d_{k+1}^T g_{k+1} = \beta_k^{BBY1}[d_k^T g_{k+1} - d_k^T y_k] = \beta_k^{BBY1} d_k^T g_k < 0. \tag{23}$$

This completes the proof.

For a study of the new algorithm's convergence, we employ assumptions on the objective function. Based on these assumptions, we establish that the new algorithm is globally convergent, as stated in the following theorem.

Theorem 3.2. Assuming that (3) determines the search direction d_{k+1}, this means that:

$$\lim_{k\to\infty} \inf \|g_k\| = 0. \tag{24}$$

Proof. Beginning with equation (3), we derive $d_{k+1} + g_{k+1} = \beta_k d_k$. Through the process of squaring each side, we ascertain:

$$\|d_{k+1}\|^2 + \|g_{k+1}\|^2 + 2d_{k+1}^T g_{k+1} = (\beta_k)^2 \|d_k\|^2, \tag{25}$$

By applying multiplication to both sides of the aforementioned equation by $\frac{1}{(d_{k+1}^T g_{k+1})^2}$, one obtains:

$$\begin{aligned}
\frac{\|d_{k+1}\|^2}{(d_{k+1}^T g_{k+1})^2} &= -\frac{2}{d_{k+1}^T g_{k+1}} - \frac{\|g_{k+1}\|^2}{(d_{k+1}^T g_{k+1})^2} + \frac{(\beta_k^{BBY1})^2 \|d_k\|^2}{(d_{k+1}^T g_{k+1})^2} \\
&\leq -\left(\frac{\|g_{k+1}\|}{d_{k+1}^T g_{k+1}} + \frac{1}{\|g_{k+1}\|^2}\right)^2 + \frac{1}{\|g_{k+1}\|^2} + \frac{\|d_k\|^2}{(d_k^T g_k)^2} \\
&\leq \frac{1}{\|g_{k+1}\|^2} + \frac{\|d_k\|^2}{(d_k^T g_k)^2},
\end{aligned} \tag{26}$$

Take note of:

$$\frac{\|d_{k+1}\|^2}{(d_{k+1}^T g_{k+1})^2} \leq \sum_{i=1}^{k+1} \frac{1}{\|g_i\|^2}, \tag{27}$$

Let us define $c_1 > 0$ such that $\|g_k\| \geq c_1$ for all $k \in \mathbb{N}$. Then,

$$\frac{\|d_{k+1}\|^2}{(d_{k+1}^T g_{k+1})^2} < \frac{k+1}{c_1^2}, \tag{28}$$

The above inequality now implies that:

$$\sum_{k=1}^{\infty} \frac{(g_k^T d_k)^2}{\|d_k\|^2} = \infty, \tag{29}$$

This leads to a contradiction with Lemma 2.1. Therefore, $\lim_{k\to\infty} \inf \|g_k\| = 0$ holds. The proofs of the other methods are similar to the approach in BBY1.

4 Numerical Experiments

In this section, we present a series of numerical results to demonstrate the effectiveness of the proposed New method in removing salt-and-pepper impulse noise from images. Our goal is to thoroughly evaluate the performance of the New method and compare it with the existing FR method under various experimental conditions.

All the programming code and its related algorithms for these experiments were created and used in MATLAB, version R2017a. Once the programming code was ready, the experiments were run on a PC with suitable specifications to run them smoothly and successfully. The numerical results are compared with standard performance measures that measure the quality of noise removal and image recovery. These results provide a clear comparison, highlighting the advantages and potential improvements offered by the New method over the FR method.

The following are the stopping criteria for both methods:

$$\frac{|f(u_k)-f(u_{k-1})|}{|f(u_k)|} \leq 10^{-4} \quad \text{and} \quad \|\nabla f(u_k)\| \leq 10^{-4}(1+|f(u_k)|) \tag{30}$$

The test images used in our experiments include widely recognized standard images such as Lena, House, Cameraman, and Elaine, along with a sample test text image. Following the approach outlined in references [29,30], we employ the Peak Signal-to-Noise Ratio (PSNR) as a quantitative metric to evaluate and compare the quality of image restoration. PSNR is a widely accepted measure that reflects the similarity between the original and the restored images, providing a clear indication of the effectiveness of noise removal. The PSNR is mathematically defined as follows:

$$\text{PSNR} = 10\log_{10}\left(\frac{255^2}{\frac{1}{MN}\sum_{i,j}(u^r_{i,j}-u^*_{i,j})^2}\right) \tag{31}$$

Here, $u^r_{i,j}$ and $u^*_{i,j}$ represent the pixel values at position (i,j) in the original and restored images, respectively, and $M\times N$ is the image dimension.

Table 1: Numerical results of FR and New algorithms.

Image	Noise level r (%)	FR-Method			BBY1-Method			BBY2-Method			BBY3-Method		
		NI	NF	PSNR (dB)	NI	NF	PSNR (dB)	NI	NF	PSNR (dB)	NI	NF	PSNR (dB)
Le	50	82	153	30.5529	55.0	69.0	30.4282	58.0	69.0	30.4360	72.0	76.0	30.4668
	70	81	155	27.4824	64.0	79.0	27.4233	50.0	60.0	27.5177	64.0	68.0	27.3287
	90	108	211	22.8583	69.0	83.0	22.7633	69.0	80.0	23.0388	107.0	214.0	23.0365
Ho	50	52	53	30.6845	33.0	42.0	34.782	48.0	55.0	34.9648	42.0	43.0	34.5528
	70	63	116	31.2564	41.0	47.0	30.5963	47.0	55.0	31.0419	48.0	50.0	30.9029
	90	111	214	25.287	70.0	80.0	24.8714	67.0	77.0	25.013	63.0	65.0	25.191
El	50	35	36	33.9129	30.0	36.0	33.8913	34.0	40.0	33.8857	34.0	36.0	33.8743
	70	38	39	31.864	39.0	47.0	31.8007	38.0	44.0	31.8211	42.0	44.0	31.7924
	90	65	114	28.2019	50.0	58.0	28.1777	50.0	58.0	28.2136	54.0	56.0	28.1106
c512	50	59	87	35.5359	39.0	50.0	35.4164	38.0	49.0	35.4281	60.0	120.0	35.5217
	70	78	142	30.6259	44.0	55.0	3.06682	47.0	54.0	30.6175	66.0	131.0	30.5963
	90	121	236	24.3962	57.0	71.0	24.9216	67.0	78.0	24.7394	70.0	72.0	24.8714

As seen from Table 1, the proposed algorithms are superior to the FR algorithm with respect to function evaluations and number of iterations and peak signal to noise ratio.

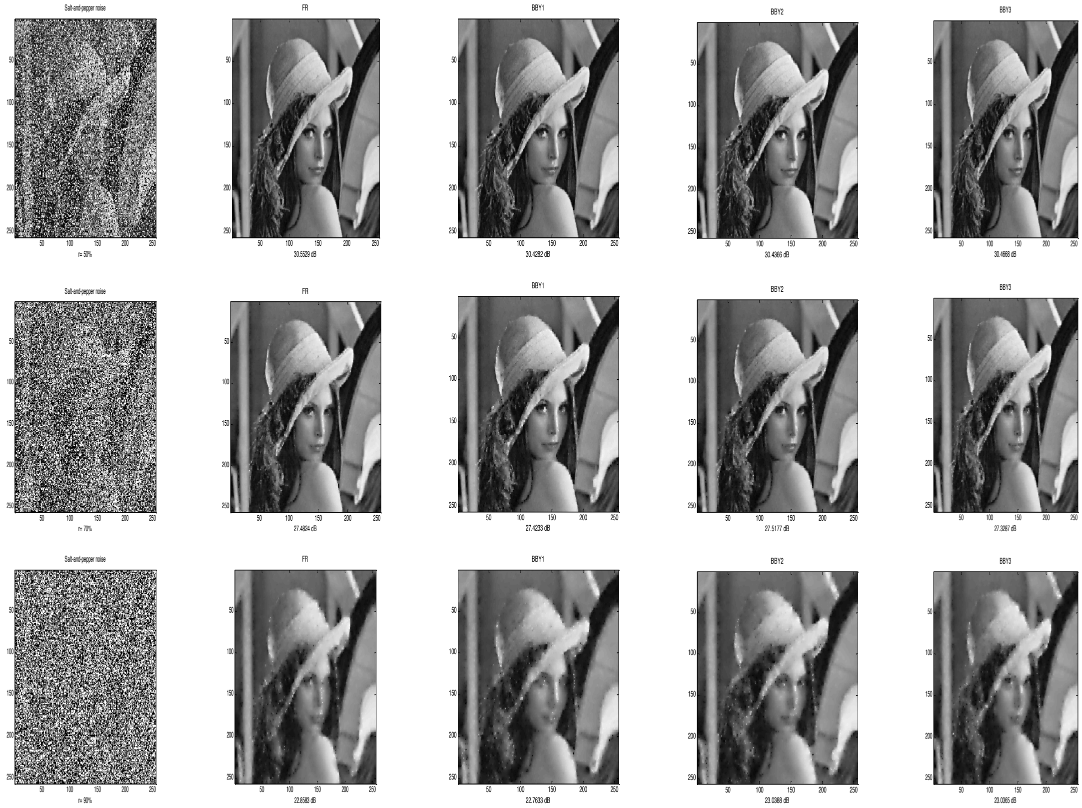

Fig. 1: Image restoration results showing original, noisy, and restored images using different methods.

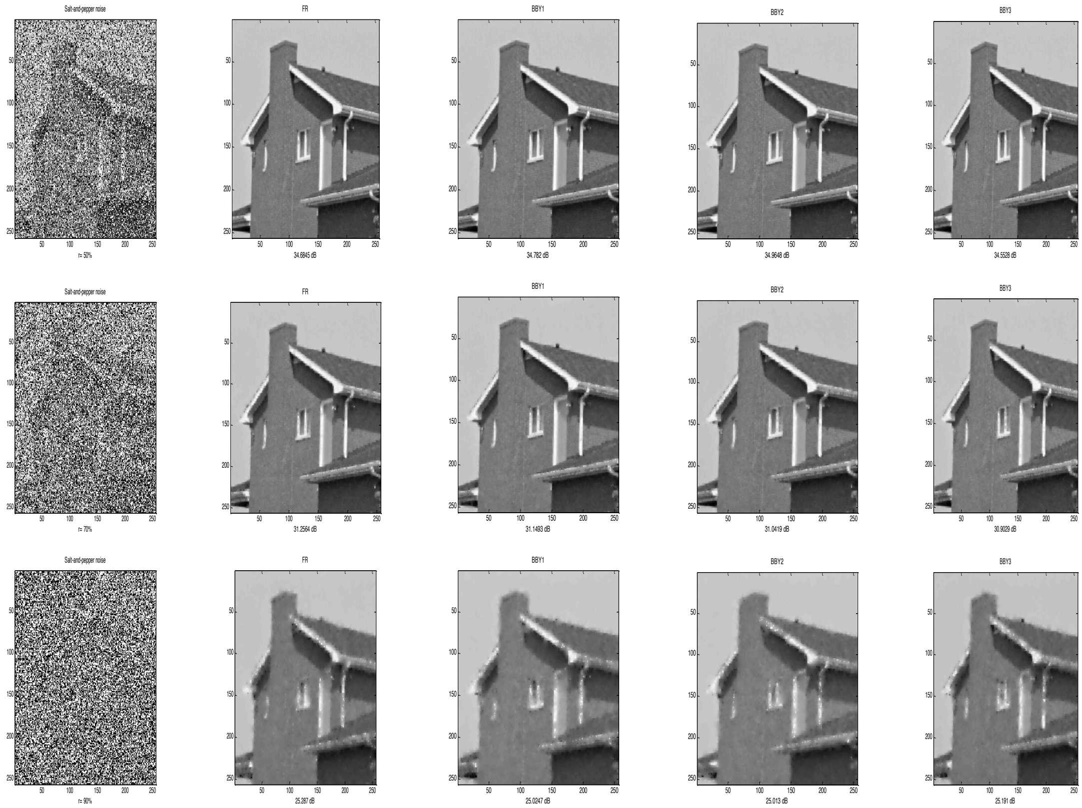

Fig. 2: Demonstrates the results of algorithms FR, BBY1, BBY2 and BBY3 of 256 × 256 House image

Fig. 3: Demonstrates the results of algorithms FR, BBY11, BBY2 and BBY3 of 256 × 256 Elaine image.

Fig. 4: Demonstrates the results of algorithms FR, BBY11, BBY2 and BBY3 of 256 × 256 Cameraman image.

article graphicx subcaption caption

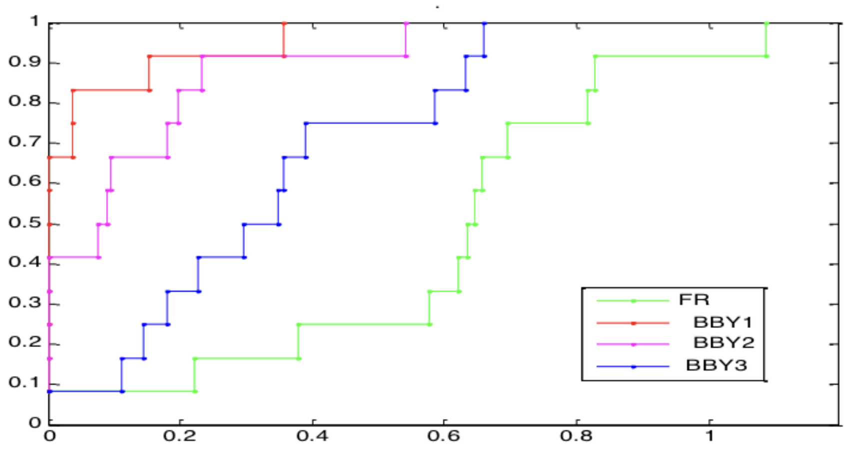

Fig. 5: Performance on the number of iterations.
This figure shows the performance profiles of the proposed BYY methods and the classical FR algorithm based on the number of iterations (NI). The proposed method outperforms the classical FR algorithm by achieving faster convergence on most test problems. Its curve rises more quickly, indicating fewer iterations are needed. In contrast, the classical FR algorithm lags behind, suggesting lower computational efficiency. The second illustrates the impact of function evaluations on computational cost. The proposed algorithm's curve (red) consistently outperforms the classical FR, requiring fewer evaluations to reach optimality. This highlights the greater efficiency of the BBY methods.

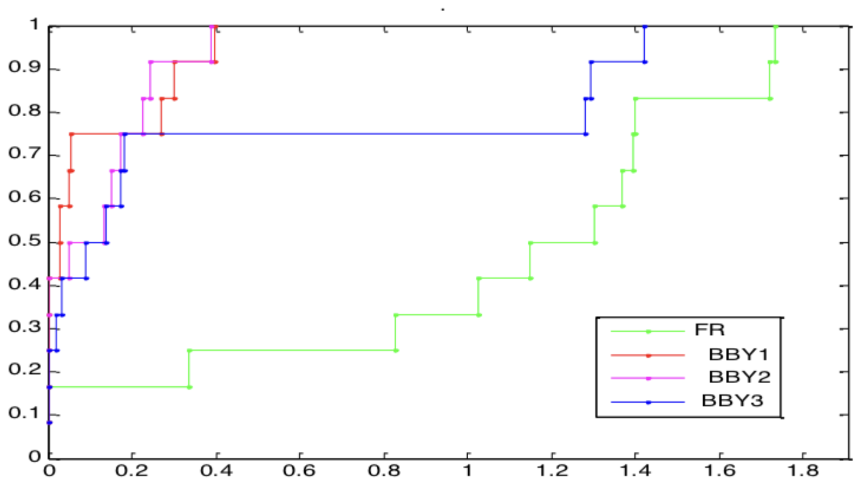

Fig. 6: Function evaluations performance.

5 Conclusion

In this paper, we introduced an efficient and complete new image restoration algorithm to remove salt-and-pepper impulse noise based on improved Conjugate Gradient (CG) algorithms. With a strong focus on classical optimization techniques, our work provides a mathematically sound framework for attaining computational efficiency with high-quality image reconstruction guarantee. More particularly, we introduced three BBY-type algorithms based on Taylor series each of which is well constructed for enhanced convergence rate without losing the critical image details like edges and textures during restoration. Adaptive in nature, the algorithms automatically adapt themselves according to varying noise levels, providing the same level of performance under all situations.

The two-stage model—integration of noise detection with adaptive median filtering and then optimization—was shown to be very effective in image restoration from noisy images and perform better compared to traditional single-stage approaches. Theoretical analysis ensured the global convergence of the BBY algorithms under reasonable assumptions, thereby their mathematical stability and validity. Furthermore, the descent direction property of the search direction was strictly established, with stable and efficient optimization in restoration.

Computational simulations verified our novel BBY approaches to outperform the traditional FR method significantly in numbers of iterations and image quality at faster convergence without sacrificing precision. The improvement was consistently shown through higher PSNR values under different levels of noise and common test images, illustrating the adaptability and stability of our approach. The experiments confirm the real-world validity, effectiveness, and scalability of the said proposed algorithms, which make them far too adequate for very noisy real-world image processing applications like medical imaging, satellite images, and surveillance systems.

Future Work: In the future, it is possible to extend such algorithms to color images, where channel interdependencies can add additional complexity, or to video restoration, where temporal consistency needs to be preserved. Another direction could be the incorporation of suggested schemes with hybrid deep-learning-based models by taking advantage of optimization-based as well as data-driven benefits for even higher quality restoration. These advances would further establish the position of our BBY algorithms within next-generation image processing pipelines.

Acknowledgment

The Researcher would like to thank the Deanship of Graduate Stuides and Scientific Research at Qassim University for financial support (QU-APC-2025).
The authors are grateful to the anonymous referee for a careful checking of the details and for helpful comments that improved this paper.

References

[1] Zhang, L., Xiong, J., Feng, Y., & Liu, J. (2023). An adaptive conjugate gradient method for impulse noise removal. *Journal of Industrial and Management Optimization*, **20**(6), 2050–2061. https://doi.org/10.3934/jimo.2023155

[2] Cai, J., Chan, R. H., & Nikolova, M. (2008). Two-phase approach for deblurring images corrupted by impulse plus gaussian noise. *Inverse Problems and Imaging*, **2**(2), 187–204. https://doi.org/10.3934/ipi.2008.2.187

[3] Hassan, B. A., Moghrabi, I. A. R., Ameen, T. A., Sulaiman, R. M., & Sulaiman, I. M. (2024). Image noise reduction and solution of unconstrained minimization problems via new conjugate gradient methods. *Mathematics*, **12**(17), 2754. https://doi.org/10.3390/math12172754

[4] Liang, H., Li, N., & Zhao, S. (2021). Salt and pepper noise removal method based on a Detail-Aware filter. *Symmetry*, **13**(3), 515. https://doi.org/10.3390/sym13030515

[5] Alajlan, N., Kamel, M., & Jernigan, E. (2004). Detail preserving impulsive noise removal. *Signal Processing: Image Communication*, **19**(10), 993–1003. https://doi.org/10.1016/j.image.2004.08.003

[6] Gonzalez, R. C., & Woods, R. E. (2018). *Digital Image Processing*. Pearson.

[7] Pitas, I., & Venetsanopoulos, A. N. (1990). *Nonlinear Digital Filters*. Springer. https://doi.org/10.1007/978-1-4757-6017-0

[8] Hestenes, M. R., & Stiefel, E. (1952). Methods of conjugate gradients for solving linear systems. *Journal of Research of the National Bureau of Standards*, **49**(6), 409–436. https://doi.org/10.6028/jres.049.044

[9] Castro, E. R., Martins, E. O., Sarthour, R. S., Souza, A. M., & Oliveira, I. S. (2024). Improving the convergence of an iterative algorithm for solving arbitrary linear equation systems using classical or quantum binary optimization. *Frontiers in Physics*, **12**. https://doi.org/10.3389/fphy.2024.1443977

[10] Saad, Y. (2003). *Iterative Methods for Sparse Linear Systems* (2nd ed.). Society for Industrial and Applied Mathematics. https://doi.org/10.1137/1.9780898718003

[11] Hassan, B. A., & Alashoor, H. A. (2022). On image restoration problems using new conjugate gradient methods. *Indonesian Journal of Electrical Engineering and Computer Science*, **29**(3), 1438–1445. https://doi.org/10.11591/ijeecs.v29.i3.pp1438-1445

[12] Fan, L., Zhang, F., Fan, H., & Zhang, C. (2019). Brief review of image denoising techniques. *Visual Computing for Industry, Biomedicine and Art*, **2**(1). https://doi.org/10.1186/s42492-019-0016-7

[13] Sun, X., Luo, H., Liu, G., Chen, C., & Xu, F. (2021). Lightweight image restoration network for strong noise removal in nuclear radiation scenes. *Sensors*, **21**(5), 1810. https://doi.org/10.3390/s21051810

[14] Hassan, B. A., & Sadiq, H. M. (2022). A new formula on the conjugate gradient method for removing impulse noise images. *Bulletin of the South Ural State University. Series: Mathematical Modelling, Programming & Computer Software*, **15**(4), 123–130.

[15] Hassan, B. A., & Sadiq, H. (2022). Efficient new conjugate gradient methods for removing impulse noise images. *European Journal of Pure and Applied Mathematics*, **15**(4), 2011–2021. https://doi.org/10.29020/nybg.ejpam.v15i4.4568

[16] Hassan, B. A., & Alashoor, H. (2022). A new type coefficient conjugate on the gradient methods for impulse noise removal in images. *European Journal of Pure and Applied Mathematics*, **15**(4), 2043–2053. https://doi.org/10.29020/nybg.ejpam.v15i4.4579

[17] Guan, S., Liu, B., Chen, S., Wu, Y., Wang, F., Liu, X., & Wei, R. (2024). Adaptive median filter salt and pepper noise suppression approach for common path coherent dispersion spectrometer. *Scientific Reports*, **14**(1). https://doi.org/10.1038/s41598-024-66649-y

[18] Hassan, B. A., & Abdullah, A. A. A. (2022). Improvement of conjugate gradient methods for removing impulse noise images. *Indonesian Journal of Electrical Engineering and Computer Science*, **29**(1), 245–251. https://doi.org/10.11591/ijeecs.v29.i1.pp245-251
[19] Souli, C., Ziadi, R., Bencherif-Madani, A., & Khudhur, H. M. (2024). A hybrid CG algorithm for nonlinear unconstrained optimization with application in image restoration. *Journal of Mathematical Modeling*, **12**(2), 301–317. https://doi.org/10.22124/JMM.2024.26151.2317
[20] Halil, I. H., Moghrabi, I. A., Fawze, A. A., Hassan, B. A., & Khudhur, H. M. (2023). A Quadratic Model based Conjugate Gradient Optimization Method. *WSEAS Transactions on Mathematics*, **22**, 925–930. https://doi.org/10.37394/23206.2023.22.101
[21] Khudhur, H. M., & Halil, I. H. (2024). Noise removal from images using the proposed three-term conjugate gradient algorithm. *Computer Research and Modeling*, **16**(4), 841–853. https://doi.org/10.20537/2076-7633-2024-16-4-841-853
[22] Nocedal, J., & Wright, S. J. (2006). *Numerical Optimization*. Springer. https://doi.org/10.1007/978-0-387-40065-5
[23] Wolfe, P. (1969). Convergence conditions for ascent methods. *SIAM Review*, **11**(2), 226–235. https://doi.org/10.1137/1011036
[24] Fletcher, R. (1964). Function minimization by conjugate gradients. *The Computer Journal*, **7**(2), 149–154. https://doi.org/10.1093/comjnl/7.2.149
[25] Großmann, M., Grunert, M., & Runge, E. (2024). A robust, simple, and efficient convergence workflow for GW calculations. *npj Computational Materials*, **10**(1). https://doi.org/10.1038/s41524-024-01311-9
[26] Huang, R., Qin, Y., Liu, K., & Yuan, G. (2023). Biased stochastic conjugate gradient algorithm with adaptive step size for nonconvex problems. *Expert Systems with Applications*, **238**, 121556. https://doi.org/10.1016/j.eswa.2023.121556
[27] Yang, Y., Liu, C., Wu, H., & Yu, D. (2024). A Distorted-Image Quality assessment algorithm based on a sparse structure and subjective perception. *Mathematics*, **12**(16), 2531. https://doi.org/10.3390/math12162531
[28] Alharbi, T., Ninh, A., Subasi, E., & Subasi, M. M. (2022). The value of shape constraints in discrete moment problems: a review and extension. *Annals of Operations Research*, **318**(1), 1–31. https://doi.org/10.1007/s10479-022-04789-y
[29] Khudhur, H. M., Hassan, B. A., & Aji, S. (2023). Superior Formula for Gradient Impulse Noise Reduction from Images. *International Journal of Applied and Computational Mathematics*, **10**(1). https://doi.org/10.1007/s40819-023-01637-w
[30] Elhamid, M. A., & Khudhur, H. M. (2024). A globally convergent of two conjugate gradient methods with application to image restoration problems. *Numerical Algebra, Control and Optimization*. https://doi.org/10.3934/naco.2024027
[31] Dolan, E. D., & Moré, J. J. (2002). Benchmarking optimization software with performance profiles. *Mathematical Programming*, **91**(2), 201–213. https://doi.org/10.1007/s101070100263

Talal Alharbi was born in Saudi Arabia. He received the M.S. degree in Pure Mathematics and the M.S. degree in Operations Research, both from the Florida Institute of Technology, Melbourne, FL, USA, and the Ph.D. degree in Operations Research from the same institution. Since joining Qassim University, Buraydah, Saudi Arabia, he has been an Assistant Professor with the Department of Mathematics, where he leads research at the intersection of optimization, artificial intelligence, and decision sciences. He has authored several high-impact publications in these areas and collaborates with both academic and industry partners. His research interests include optimization, operations research, simulation, stochastic programming, applied mathematics, operations management, decision making, fuzzy logic, graph theory, neural networks, artificial intelligence, the Internet of Things (IoT), and statistical modeling. Dr. Talal is an active member of several professional organizations, including the Stochastic Programming Society (SPS), the National Training and Simulation Association (NTSA), the Modeling, Simulation, and Training Community, the INFORMS Optimization Society, and the Mathematical Optimization Society (MOS). Ta.alharbi@qu.edu.sa .

Basim A. Hassan is currently a Professor in Department of Mathematics, College of Computer Science and Mathematics, University of Mosul. He obtained his M.Sc and Ph.D degrees in Mathematics from the University of Mosul, in 2000 and 2010, respectively with specialization in optimization. To date, he has published more than 80 research paper in various international journals and conferences. He currently works on iterative methods. His research interest in applied mathematics, with a field of concentration of optimization include conjugate gradient, steepest descent methods, Broyden's family and quasi- Newton methods with application in signal recovery and image restoration. He can be contacted at email: basimah@uomosul.edu.iq.